USING DUAL-WAVELENGTH FIBER BRAGG GRATINGS FOR TEMPERATURE AND STRAIN SENSING AT CRYOGENIC TEMPERATURE*

Meng-Chou Wu, William H. Prosser, Robert S. Rogowski, and Stanton L. DeHaven

NASA, Langley Research Center
MS 231
Hampton, VA, USA 23681-2199

ABSTRACT

By using dual-wavelength fiber-optic Bragg gratings, a new technique has been developed for sensing both temperature and strain simultaneously in cryogenic temperature range. Two Bragg gratings with different wavelengths were inscribed at the same location in an optical fiber to form a dual-wavelength sensor. By measuring the wavelength shifts that resulted from the fiber being subjected to different temperatures and strains, the wavelength-dependent thermo-optic coefficients and photoelastic coefficients of the fiber were determined. These coefficients were used to construct the elements of the K matrix, which enables to determine inversely the strain and temperature changes by measuring the wavelength shifts of the dual-wavelength Bragg grating. In this study, measurements were made over the temperature range from room temperature down to about 10 K, addressing much of the low temperature range of cryogenic tanks. A structure transition of the optical fiber during the temperature change was found from about 70 K to 140 K. This transition caused splitting of the waveforms characterizing the Bragg gratings, and the determination of wavelength shifts was consequently complicated. Several alternatives are proposed to resolve this problem. The effectiveness and sensitivities of these measurements in different temperature ranges are discussed. The separation of two wavelengths for the dual-wavelength Bragg grating has been widened to increase the sensitivities of measurement; however, this separation can still be covered in the scanning range from a single scanning laser.

INTRODUCTION

Fiber Bragg gratings (FBGs) have been widely used as strain sensors in aerospace applications, as well as in other fields.[1-3] Compared with conventional strain gauges, FBG strain sensors have similar sensitivity but are much lighter in weight and require simpler wiring. These advantages are especially important for aerospace applications. However, FBGs are also sensitive to temperature changes. Thermally induced wavelength shifts of a FBG are indistinguishable from those induced by strain within a simple strain measurement. This technical issue can be relatively serious when the measurements are conducted in an environment with large temperature gradients or fluctuations, for example, on the surface of cryogenic fuel tanks employed in aerospace vehicles. In these cases temperature compensation is necessary for strain measurements. There have been several techniques developed for intrinsic temperature compensation.[4-8] Xu et al.[4] have demonstrated a method using dual-wavelength gratings to simultaneously measure temperature and strain. In this method a sensing element contains two superimposed FBGs, written at 850 nm and 1300 nm. The thermo-optic coefficients and photoelastic coefficients are wavelength-dependent and the large center wavelength separation therefore allows differentiating between the thermal and strain effects. Nevertheless this technique requires two broadband light sources and two detecting systems. This requirement might be impractical for some aerospace applications.

Further, most techniques for temperature compensation address temperature ranges only around and above room temperature. Few investigate the lower temperature range, for example, of cryogenic tanks.[9] To the best of our knowledge, a complete picture for simultaneous strain and temperature sensing is still not available. In this study we investigate the feasibility of cryogenic applications using dual-wavelength FBGs for strain/temperature discrimination. The gratings were written around 1550nm with a separation

---

* Distribution statement A: Approved for public release; distribution is unlimited.

of 30 nm, such that only a single scanning laser is required for the experiment. Measurements were made over the temperature range from room temperature down to about 10 K, addressing much of the low temperature range of cryogenic tanks.

THEORY

When using FBG sensors in measurements of strain or temperature, it is assumed that the Bragg wavelength shifts $\Delta\lambda_\varepsilon$ and $\Delta\lambda_T$ are linear in response respectively to a strain change $\Delta\varepsilon$ and a temperature change ΔT and can therefore be expressed in the form

$$\begin{aligned}\Delta\lambda_\varepsilon &= K_\varepsilon \Delta\varepsilon \\ \Delta\lambda_T &= K_T \Delta T\end{aligned} \tag{1}$$

for small perturbations, where K_ε and K_T are the strain and temperature coefficients respectively. K_ε is determined by the Poisson ratio of the fiber, the photoelastic coefficient and the effective refractive index of the fiber core, and K_T by the thermal expansion coefficient and the thermo-optic coefficient. In general, a Bragg wavelength shift is a linear combination of strain and temperature, that is,

$$\Delta\lambda_B\,(\varepsilon,\, T) = K_\varepsilon \Delta\varepsilon + K_T \Delta T. \tag{2}$$

It is also assumed that these individual terms are independent. That is, the related strain-temperature cross-term is negligible, a phenomenon which applies well for small perturbations. For two Bragg wavelength shifts to be observed, the resulting two equations can be expressed in a matrix form,

$$\begin{bmatrix}\Delta\lambda_{B1} \\ \Delta\lambda_{B2}\end{bmatrix} = \begin{bmatrix}K_{1\varepsilon} & K_{1T} \\ K_{2\varepsilon} & K_{2T}\end{bmatrix}\begin{bmatrix}\Delta\varepsilon \\ \Delta T\end{bmatrix}. \tag{3}$$

The elements of this 2 x 2 $\boldsymbol{K}$ matrix can be determined by measuring each Bragg wavelength shift with strain and temperature separately. With the constructed matrix, the changes of temperature and strain can be calculated by experimentally measuring both of the Bragg wavelength shifts. This can be expressed as the inverse of Eq. (3),

$$\begin{bmatrix}\Delta\varepsilon \\ \Delta T\end{bmatrix} = C\begin{bmatrix}K_{2T} & -K_{1T} \\ -K_{2\varepsilon} & K_{1\varepsilon}\end{bmatrix}\begin{bmatrix}\Delta\lambda_{B1} \\ \Delta\lambda_{B2}\end{bmatrix}, \tag{4}$$

where $C = 1/(K_{1\varepsilon}K_{2T} - K_{2\varepsilon}K_{1T})$. The inverse of matrix $\boldsymbol{K}$ exists only if the determinant of $\boldsymbol{K}$ is nonzero and therefore the ratio of the strain responses of two gratings must be different from the ratio of their temperature responses, i.e., $K_{1T}/K_{2T} \neq K_{1\varepsilon}/K_{2\varepsilon}$.

EXPERIMENT

A pulsed Excimer laser of 248 nm and a Talbot interferometer arrangement were used to write the dual-wavelength FBGs, as shown in Figure 1. Both standard telecommunication fiber and boron-germanium co-doped photosensitive fiber were used. The wavelengths of gratings were adjusted by changing the relative angle of the two mirrors in the interferometer. For writing a dual-wavelength grating, two gratings were superimposed and their wavelengths were maintained around 1550 nm with a separation of about 30 nm. Typical exposure was a 20 Hz pulse rate for a duration of less than 1 minute. This produced gratings with relatively low reflectivities, which might be difficult to be monitored with a conventional optical spectrum analyzer.

The low reflectivity gratings were interrogated by using a frequency domain demodulation system[10], shown in Figure 2. In this system, the fiber coupler C_1 and a pair of Faraday rotation mirrors (FRMs) form an in-fiber interferometer with an optical path difference of $2n_{eff}L_0$, where n_{eff} is the effective refractive index of the fiber core and L_0 the length of the reference cavity. The signals are driven by the tuning of the laser and detected at the photo-detector D_1. They are used to trigger the sampling of signal at D_2, which is the output of another in-fiber interferometer formed with the fiber coupler C_2, a broadband reflector, and a particular fiber Bragg grating at a distance of L_i. A series of low reflectivity Bragg gratings can be written at the same wavelength on a single fiber at different locations and the reflected signals are superimposed and detected at D_2.

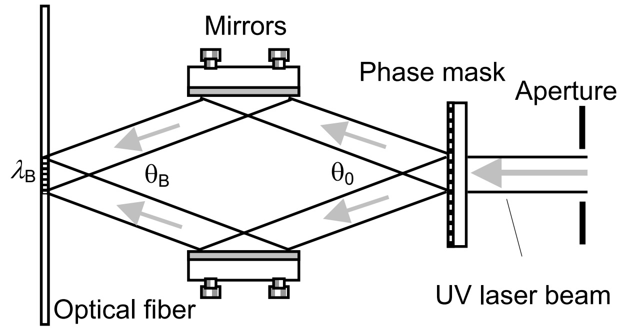

Figure 1. Schematic representing the interferometric technique for generating fiber Bragg gratings. The Bragg wavelength λ_B is determined by the adjustable θ_B.

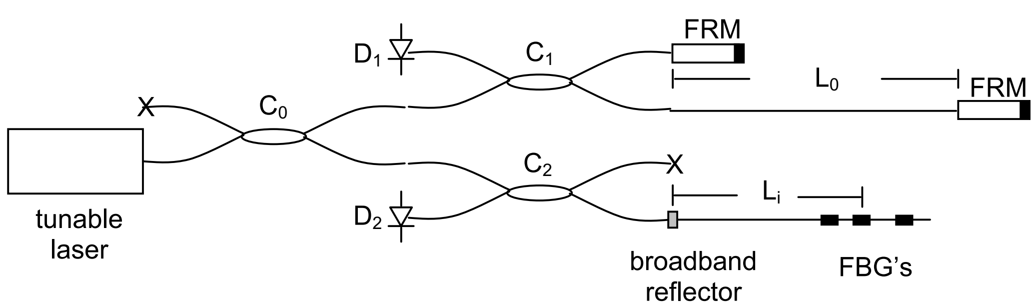

Figure 2. Schematic diagram of a frequency domain demodulation system. Items C_0, C_1, and C_2 are fiber couplers. "X" indicates that the unused port is terminated. Items D_1 and D_2 are detectors and FRMs a pair of Faraday rotation mirrors.

The detected signals are further processed (fast-Fourier-transformed) to display the spatial spectrum, which shows the distances and physical profiles of the gratings. The spectrum of a particular grating can then be windowed and inverse-fast-Fourier-transformed to get its wavelength spectrum. Shown in Figure 3(a) is the spatial spectrum of a typical FBG with a physical length of about 3 mm and (b) its wavelength spectrum, which can be used for strain and temperature sensing. In Figure 4(a), the spatial spectrum of a dual-wavelength Bragg grating shows the characteristics of interference by two superimposed gratings. Figure 4(b) shows the wavelength spectrum of this dual-wavelength Bragg grating, with nominal Bragg wavelengths of ~1536 nm and ~1564 nm.

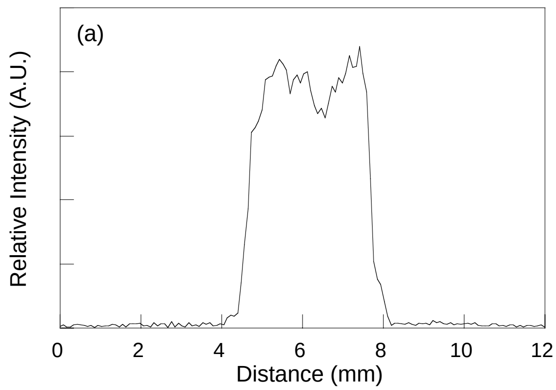

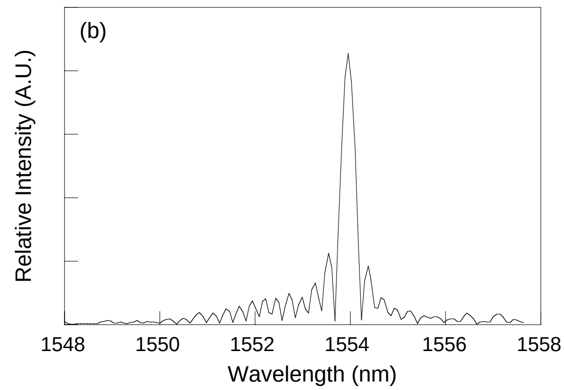

Figure 3. (a) Spatial spectrum and (b) wavelength spectrum of a written Bragg grating with a physical length of about 3 mm and a center wavelength of 1554 nm.

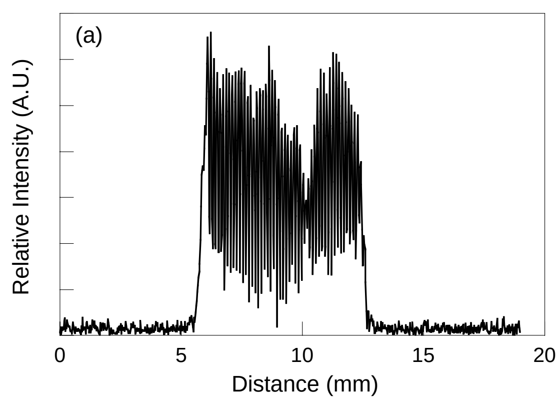

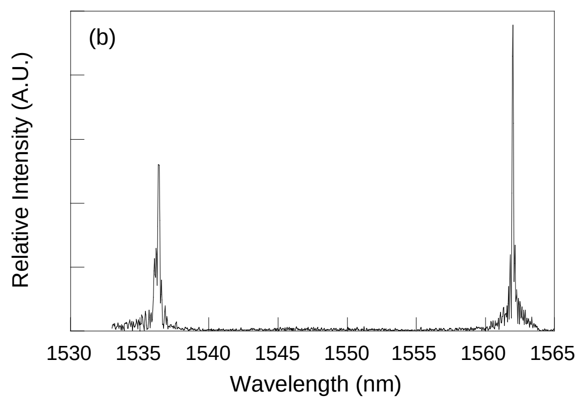

Figure 4. (a) Spatial spectrum and (b) wavelength spectrum of a dual-wavelength Bragg grating with nominal Bragg wavelengths of about 1536 nm and 1564 nm.

A cryostat of compressed helium gas was used for temperature control. After the gratings had been written, the stripped portion of the optical fiber was not recoated and directly attached to the cold plate in the cryogenic chamber. This ensured that all the thermal effects were resulting only from the fiber and not the coating polymer. Temperature was varied from slightly above room temperature down to about 10 K and controlled within 0.05 K. The center wavelengths were monitored using the processed signals from the frequency domain demodulation system described above, with a resolution of 0.02 nm.

The strain tests were conducted at room temperature (295 K). The optical fiber with a dual-wavelength grating was bonded to two 10 cm long aluminum plates spaced 30 cm apart. The bonding portion on each plate had a length of 5 cm. The grating was centered 15 cm from each plate. The strain was applied to the fiber by pulling the two aluminum plates for a range of 0 - 6700 μstrain.

RESULTS AND DISCUSSION

Figure 5 and Figure 6 show the temperature responses of Bragg gratings. It is clear that the thermally-induced wavelength shifts are relatively linear from 310 K down to 160 K, although there are a few slight changes of gradients within this temperature range. This result of linearity in a finite range is consistent with the assumption that the temperature coefficient is linear for small perturbations.

Figure 7(a) and (b) show the linear curve fitting of the thermal responses at two Bragg wavelengths for the temperature range from 244 K to 312 K. The measured temperature coefficients were

$$K_{1T} = 8.07 \pm 5.4 \times 10^{-2} \text{ pm/}^\circ\text{C}$$
$$K_{2T} = 8.30 \pm 5.0 \times 10^{-2} \text{ pm/}^\circ\text{C}$$

where the temperature scale was converted to conventional degree Celsius. It should be noted that these values are of bare fibers without the contribution of coating materials, as mentioned in the previous section.

From 150 K to 80 K, the changes are more complicated. The original well-defined center peak of the Bragg wavelength is split. The determination of the wavelength shift is therefore more difficult, if not impractical. This behavior is possibly due to the structural transition of germanium-induced defect levels. Further investigation needs to be done. As the temperature approaches the transition temperature, the nonlinearity of the responses makes the dual-wavelength Bragg gratings impractical for the measurement of temperature.

For the temperature range from 80 K to 10 K, the Bragg wavelength has practically no thermally-induced changes, due to extremely low thermal expansion coefficient and thermo-optic coefficient. It is obviously impossible to use the dual-wavelength Bragg gratings to determine the temperature. However, in this temperature range, the wavelength shifts can be totally attributed to the effect of strain, i.e., strains can be measured without the corrections for temperature. It should be noted that the same thermal behaviors were also seen for a single Bragg grating for the whole temperature range.

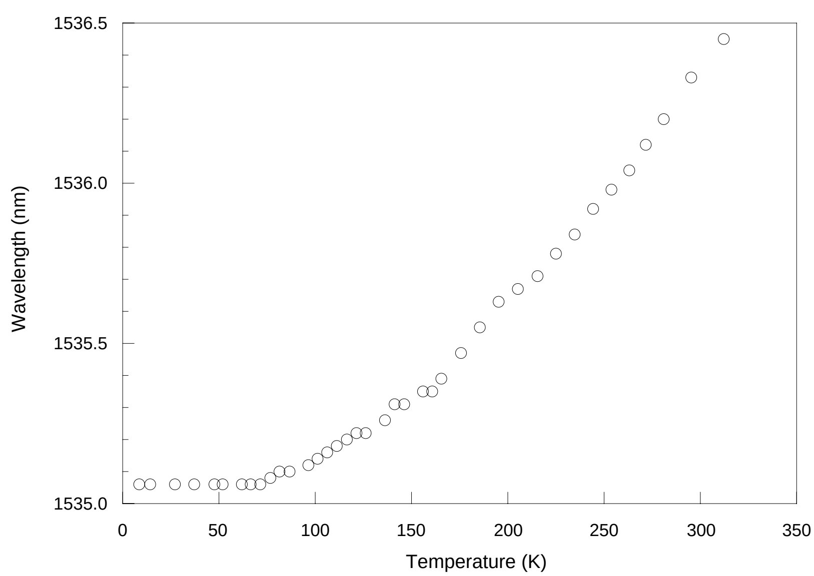

Figure 5. Temperature response of the Bragg grating with a nominal wavelength of 1536 nm.

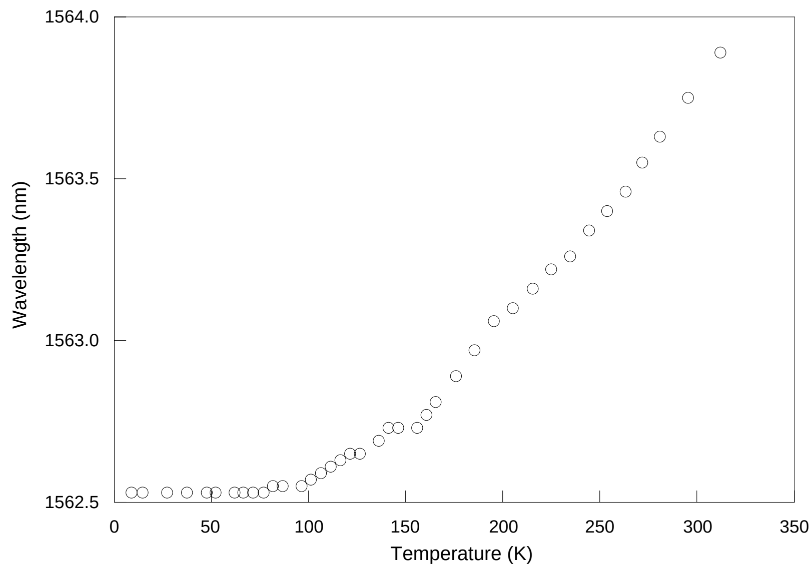

Figure 6. Temperature response of the Bragg grating with a nominal wavelength of 1564 nm.

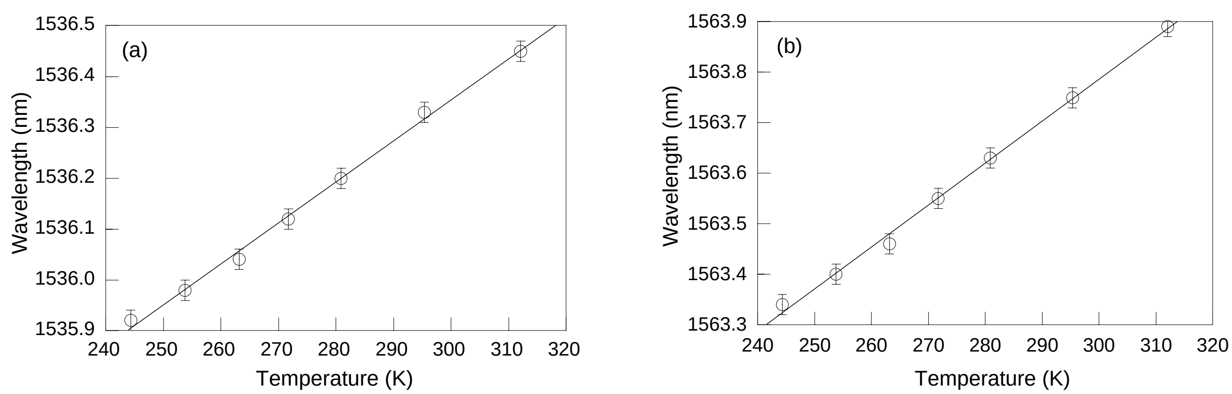

Figure 7. Linear curve fitting of the thermal responses at two Bragg wavelengths for the temperature range from 244 K to 312 K.

Figure 8(a) and (b) show the strain-induced wavelength shift at two nominal Bragg wavelengths. The measured values of the two strain coefficients were

$$K_{1\varepsilon} = 1.159 \pm 3.1 \times 10^{-3} \text{ pm}/\mu\text{strain}$$
$$K_{2\,\varepsilon} = 1.168 \pm 3.6 \times 10^{-3} \text{ pm}/\mu\text{strain}.$$

These and two previously shown temperature coefficients combine to form a nonzero determinant of ***K*** matrix. Therefore the inverse matrix can be used to determine temperature and strain simultaneously from the wavelength measurements. However the current wavelength separation of the grating can be further increased to give well-separate coefficients and to decrease errors for the determination of temperature and strain.

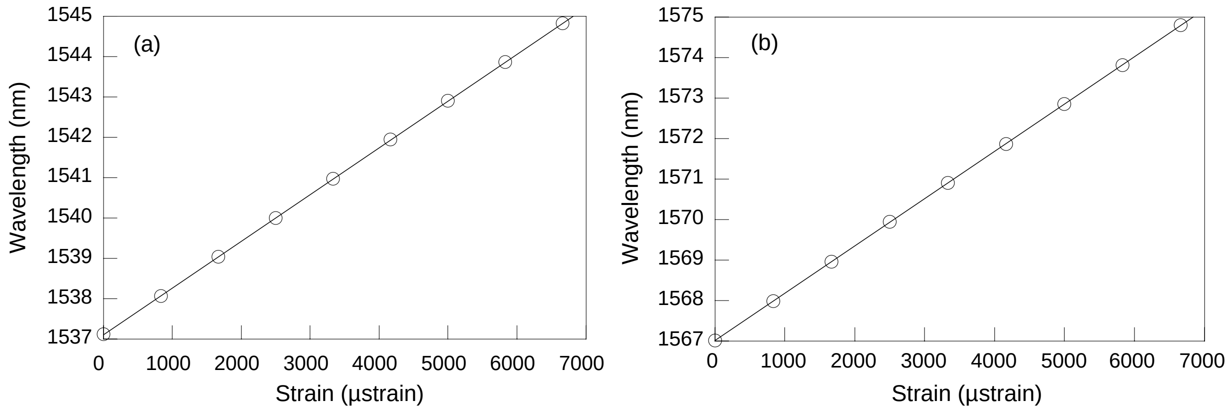

Figure 8. Strain response of the dual-wavelength Bragg grating.

SUMMARY AND CONCLUSIONS

A new technique, using low reflectivity FBGs for strain/temperature discrimination, is demonstrated. In this study, measurements were made over the temperature range from room temperature down to about 10 K, addressing much of the low temperature range of cryogenic tanks. Linear thermal responses of these gratings were found in the higher temperature range. A possible structural transition of the optical fiber was found as the temperature decreased. This transition caused splitting of the waveforms characterizing the Bragg gratings, and the determination of wavelength shifts was consequently complicated. For temperatures lower than 90 K, the temperature coefficients of FBGs were found to be practically zero and hence strains can be measured without temperature compensations. Two distinguishable strain coefficients are also obtained at two nominal Bragg wavelengths from the strain tests. Further increase of the separation will be pursued to decrease the errors for the prediction of strain and temperature.

REFERENCES

1. C. R. Giles, ***Lightwave applications of fiber Bragg gratings***, J. Lightwave Technol. **15**, 1391-1404 (1997).

2. K. O. Hill, Y. Fujii, D. C. Johnson, and B. S. Kawasaki, ***Photosensitivity in optical waveguides: application to reflection filter fabrication***, Appl. Phys. Lett. **32**, 647-649 (1978).

3. A. D. Kersey, M. A Davis, H. J. Patrick, M. LeBlanc, K. P. Koo, C. G. Askins, M.A. Putnam, E. J. Friebele, ***Fiber grating sensors***, J. Lightwave Technol. **15**, 1442-1463 (1997).

4. M. G. Xu, J.-L. Archambault, L. Reekie, and J. P. Dakin, ***Discrimination between strain and temperature effects using dual-wavelength fiber grating sensors***, Electron. Lett. **31**, 823-825 (1994).

5. S. W. James, M. L. Dockney, and R. P. Tatum, ***Simultaneous independent temperature and strain measurement using in-fiber Bragg grating sensors***, Electron. Lett. **32**, 1133-1134 (1996).

6. H. J. Patrick, G. M. Williams, A. D. Kersey, and J. R. Pedrazzani, ***Hybrid fiber Bragg grating/long period fiber grating sensor for strain/temperature discrimination***, IEEE Photon. Technol. Lett. **8**, 1223-1225 (1996).

7. S. E. Kannellopoulos, V. A. Handrek, and A. J. Rogers, ***Simultaneous strain and temperature sensing with photogenerated in-fiber gratings***, Optic. Lett. **20**, 333-335 (1995).

8. G. P. Brady, K. Kalli, D. J. Webb, D. A. Jackson, L. Reekie, an J.-L. Archambault, ***Simultaneous measurement of strain and temperature using the first- and second-order diffraction wavelengths of Bragg gratings***, IEE Proc.-Optoelectron. **144**, 156-161 (1997).

9. S. W. James, R. P. Tatam, A. Twin, M. Morgan, and P. Noonan, ***Strain response of fiber Bragg grating sensors at cryogenic temperatures***, Meas. Sci. Technol. **13**, 1535-1539 (2002).

10. M. Froggatt and J. Moore, ***Distributed measurement of static strain in an optical fiber with multiple Bragg gratings at nominally equal wavelengths***, Appl. Opt. **37**, 1741-1746 (1998).